ACS OMEGA

http://pubs.acs.org/journal/acsodf

Article

Coexistence of Different Growth Mechanisms of Sodium Chlorate under the Same Experimental Conditions

Mićo M. Mitrović,* Biljana Z. Maksimović, Branislava M. Vučetić, Milica M. Milojević, and Andrijana A. Žekić

Cite This: *ACS Omega* 2021, 6, 21909−21914

Read Online

ACCESS | Metrics & More | Article Recommendations

ABSTRACT: Dependence of growth rates of {100} sodium chlorate crystal faces on solution supersaturation in the range of 0.44−1.32% was analyzed. It has been shown that the growth rate dispersion does not have a consequence only in the growth parameter differences predicted by specific crystal growth theory but that individual crystal faces may grow with different mechanisms under the same experimental conditions. The majority of the observed {100} sodium chlorate crystal faces grew in accordance with the power law $R \sim \sigma^n$, whereas approximately one-third of them grew in accordance with BCF or Chernov's theories. Possible reasons for this as well as for the coexistence of crystal faces, which grew with different mechanisms under the same conditions, have been discussed.

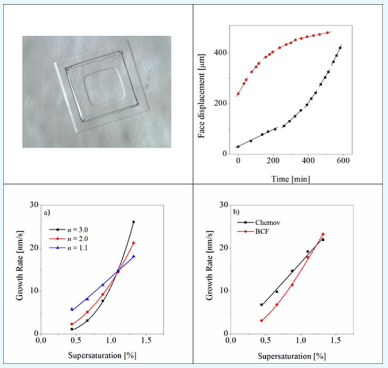

INTRODUCTION

Different competitive growth mechanisms, which depend on supersaturation and temperature, cause possible crystal growth regimes. In an attempt to make a clear determination of the mechanism responsible for crystal growth under certain conditions, many difficulties have arisen. One of the most commonly used method to identify the growth mechanism is to study (R,σ) dependence, i.e., crystal growth rate, R, on solution supersaturation, σ, dependence.

In previous analysis, the authors have tested (R,σ) dependence by using several theoretical equations. Linear dependence was found for potassium alum crystals grown at small supersaturations, while for higher supersaturations, some points lay above the linear curve,[1] as well as for the growth of hydroxyapatite in the supersaturation range of 2.05−4.58%.[2] The growth rates of potash alum crystals were fitted to equations corresponding to BCF theory, the polynuclear model, and the power law.[3] The data obtained for potassium alum crystals (supersaturation range of 2−18%) were all fitted to the BCF model.[4] Kim and Myerson fitted the experimental data of other authors with a simple semi-empirical power law equation.[5]

Under different growth conditions, (R,σ) dependence for sodium chlorate crystals is found to be nearly parabolic in the supersaturation range of $(0.3−5.0) \times 10^{-2}$% and linear in the range of $(5−15) \times 10^{-2}$%.[1] In the supersaturation range of 0.1−1.0%, the (R,σ) dependence could be parabolic or linear,[6] while in the range of 3−5%, it refers to a two-dimensional nucleation mechanism.[7] Surender et al. claimed that in the supersaturation range of 3−8% a parabolic trend emerged.[8]

Some information about the growth mechanisms of sodium chlorate crystals was obtained by the analysis of (R,σ) dependence,[9] where R corresponds to the maximum of the normal distribution describing the crystal growth rate dispersion. Consequently, only the most probable behavior of the crystals was analyzed. It is shown that the {100} sodium chlorate crystal faces, in the supersaturation range of 0.44−1.56%, predominantly grew according to BCF theory. It is shown that when supersaturation decreases, (R,σ) dependence is nearly parabolic, while when supersaturation increases, this dependence is almost linear, from which it is presumed that the growth mechanism probably depended on the solution history.

Growth rate dispersion (GRD), occurring for various substances,[1,10−23] is well-known but is not a satisfactorily explained phenomenon in crystal growth. It occurs when crystals of the same material grew at different rates under the same experimental conditions. Namely, GRD is a consequence of different behaviors of individual faces, usually explained by the differences in parameters describing the configuration of dominant dislocation groups on faces, lattice strain,[14] electrical

Received: April 23, 2021
Accepted: August 11, 2021
Published: August 20, 2021

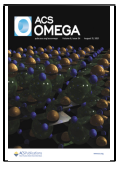

charge of face,[24] and the presence of impurities for individual faces.

Because of GRD, the analysis of (R,σ) dependence is additionally complicated. Earlier investigations of (R,σ) dependence were performed at one or only several crystals.[1−8,25] The most probable behavior of many individual {100} crystal faces of sodium chlorate was recently analyzed.[9]

In order to investigate the possibility of the coexistence of different growth mechanisms under the same experimental conditions, as a cause of growth rate dispersion, (R,σ) dependence was analyzed for numerous individual {100} sodium chlorate $NaClO_3$ (space group $P2_13$) crystal faces, and the results of this analysis will be presented in this paper.

EXPERIMENTAL RESULTS

Primary nucleated sodium chlorate crystals grew until they reached a certain size and then partially dissolved.[9] After dissolution and refaceting, a broad dispersion of sodium chlorate {100} face growth rates occurred as was previously noticed.[26,27] Also, it was remarked that growth and dissolution of sodium chlorate crystals did not depend on their position in the bottom of the crystallization cell, crystal orientation in respect to the solution flow, and the distance between the closest neighbors, i.e., they did not depend on hydrodynamic conditions. Histograms representing changes in GRD of sodium chlorate {100} faces in the experiments with the temperature increasing from 28.0 to 30.0 °C and with the temperature decreasing from 30.0 to 28.0 °C were published earlier.[9]

To determine the mechanism of crystal growth under certain conditions, the most appropriate correlation between growth rates and solution supersaturation must be found. For this reason, experimental data obtained for each individually observed face were fitted to equations corresponding to different growth mechanisms. The data were fitted to the following equations:

(1) Two-dimensional nucleation with (a) surface diffusion $R = hAC\sigma^{1/2} \exp(-\Delta G_p^*/kT)$ and (b) direct integration of growth units $R = hAC'\sigma^{1/2} \exp(-\Delta G_p^*/kT)$ (both for the polynuclear model).

(2) Two-dimensional nucleation with (a) surface diffusion $R = hB\sigma^{5/6} \exp(-\Delta G_p^*/3kT)$ and (b) direct integration of growth units $R = hB^*\sigma^{5/6} \exp(-\Delta G_p^*/3kT)$ (both for the multiple nuclear model).

(3) Growth by group cooperating screw dislocations—the Chernov's model,[28]

$$\frac{\sigma^2}{R} = \frac{19\gamma\Omega}{kT}\frac{1}{mh\Omega N_0\beta_l^*} + \frac{2L\sigma}{mh\Omega N_0\beta_l^*};$$

(4) Spiral growth−BCF,[29−32] $R = C^*\frac{\sigma^2}{\sigma_c}\tanh\left(\frac{\sigma_c}{\sigma}\right)$;

(5) Spiral growth−diffusion regime,[33] $R = \frac{C_1\sigma^2}{\ln\left[\frac{C_2}{\sigma}\sinh\left(\frac{\sigma}{C_3}\right)\right]}$;

(6) Linear (R,σ) dependence for $\sigma \gg \sigma_c$, $R = C^*\sigma$.

(7) Parabolic (R,σ) dependence for $\sigma \ll \sigma_c$, $R = C^*\frac{\sigma^2}{\sigma_c}$.

(8) Simple power law,[34] $R = K\sigma^n$.

Linear (6) and parabolic (7) dependences are predicted with all three mechanisms described by equations (3−5). Because of that, these dependences are analyzed separately.

Three versions of growth by two-dimensional nucleation are possible depending on the nuclei steps displacement rate v: (a) mononuclear for $v = \infty$, (b) polynuclear for $v = 0$, and (c) finite v (birth and spread model, also called the multiple nucleation model). In the case of finite-step velocity v, there are two models: polynuclear and multiple nucleation. For the face area A, nuclei step height h, and rate of two-dimensional nucleation J, the polynuclear model exists if $A^{1/2} < (v/J)^{1/3}$ i.e., $R = hAJ$, whereas the multiple nucleation model exists if $A^{1/2} > (v/J)^{1/3}$, i.e., $R = hJ^{1/3}v^{2/3}$. The main differences between equations for R for surface diffusion and direct integration of growth units lie in expressions for J and v, which are different in these two cases. Equations that describe polynuclear and multiple nuclear models with surface diffusion and with direct integration of growth units are essentially the same. Both models predict for low σ exponential supersaturation dependence and for high σ, $R \propto \sigma^{1/2}$ or $R \propto \sigma^{5/6}$. In the polynuclear model, the growth rate R increases with the area of the growing crystal and it is expected that the exponent exceeds 1/2 because of the surface area A contribution.[34]

Spiral growth models consider that steps on a growing surface are provided by the presence of a screw dislocation. Bulk diffusion models (3) compared to surface diffusion model (4) assumed that the diffusion of growth units in the bulk medium is slower than their diffusion on the surface and integration in the kinks. Parameters in equation 4 are defined as $C^* = \frac{\beta\Lambda\Omega N_0}{b}\beta_l^*$ and $\sigma_c = \frac{9.5\gamma\Omega}{kT\lambda_s}$, where β is the kink retardation factor (describes the influence of kinks in the steps), Λ is step retardation factor (describes the influence of kinks on the density of steps), and b is the size of the growth unit in the y direction. For the diffusion regime, $\frac{D_s}{\lambda_s} \ll \beta_l^*$—velocity of the step advance will be determined by the process of surface diffusion, i.e., surface diffusion is the rate controlling process, where β_l^* is the kinetic coefficient of the step (rate of crystallization) and D_s is the diffusion coefficient.

The goodness of equation fit was tested by the χ^2 (chi-square) test.[35]

We note that the dislocation growth mechanism is described with different equations, which the authors used in order to describe this mechanism better.[36] The majority of them are generalizations of eqs 3 and 4. The BCF equation in the original version is derived for crystal growth from vapor, but it is shown that it describes well growth from solutions (and melts).[37]

A more general model employing the BCF growth mechanism combines surface and bulk diffusion and considers these effects in parallel or series on the crystal growth rate. These models are mathematically complex and are described in detail in the literature.[31,38] The mentioned models predict that as the relative velocity between a crystal and the solution is increased, the growth will increase to a maximum value and then will remain the same. This maximum value is the value obtained when only surface diffusion limits growth. In the literature, this is known as a growth limited by interfacial attachment kinetics. When the crystal growth rate can be changed by changing the hydrodynamic conditions, it is known as a mass transfer limited growth.[36]

An example of the {100} face displacement versus time dependence of sodium chlorate crystals when supersaturation decreases and increases is presented in Figure 1. In order to determine the corresponding average linear face growth rates after refaceting, the data corresponding to constant supersaturation were subjected to the least-squares method. Some crystals changed their growth rates during the observation

https://doi.org/10.1021/acsomega.1c02150
ACS Omega 2021, 6, 21909−21914

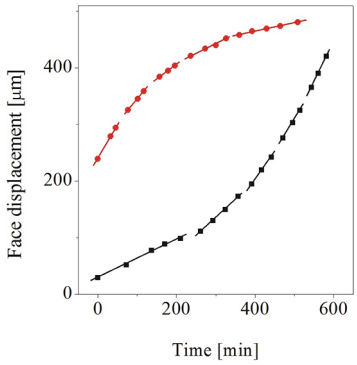

Figure 1. Sodium chlorate crystal {100} face displacement versus time dependence for a supersaturation decrease (dots) and increase (squares).

(approximately 1%), even though the supersaturation of the solution was constant, as described in ref 9. Those crystals were excluded from the analysis.

The examples of (R,σ) functions that best fit certain experimental data are presented in Figure 2.

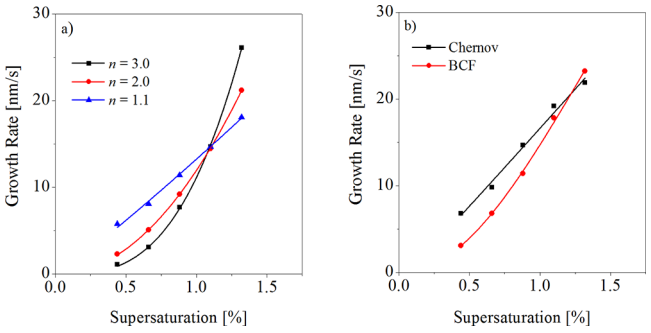

Figure 2. Experimental data for sodium chlorate crystals fitted by: (a) power function, $R = K\sigma^n$, with n = 1.1, 2.0, and 3.0 and (b) by Chernov and BCF functions.

Table 1 shows the numbers of {100} sodium chlorate crystal faces, whose growth is best described by some of the proposed equations, for both types of experiments—with supersaturations decreasing (σ_d) and increasing (σ_i). N denotes the total number of observed crystal faces. The analysis was done only for crystals whose growth could be observed at all five values of supersaturations (not intergrown).

From Table 1, one may notice that most of the sodium chlorate {100} face growth rate versus supersaturation dependences can be best described by power functions $R \sim \sigma^n$ (6, 7, 8). In Figure 3, histograms representing the power (n) distribution are presented.

The data for sodium chlorate crystals, presented in Table 1 and Figure 3, were obtained by analyzing the experimental results partially published previously.[9] Figure 3 shows the histograms of the obtained power n in experiments.

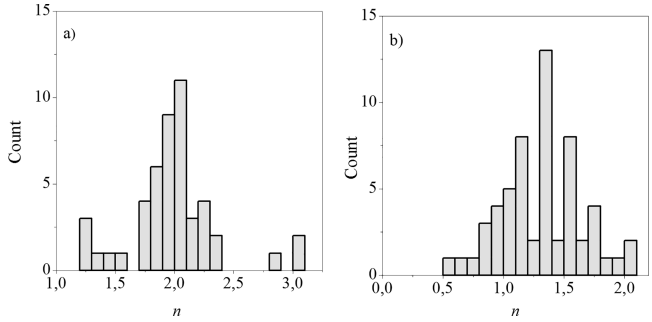

Figure 3. Distribution of power n for sodium chlorate {100} faces when (a) supersaturation decreases and (b) supersaturation increases.

DISCUSSION

It is shown that in the same experimental conditions, individual {100} sodium chlorate crystal faces grew at different rates.[9] Many crystal faces did not grow at all, which confirms the occurred stability of non-growing crystal faces at relatively high solution undercooling (to 13 °C).[27] The existence of zero growth rates probably depended on the proximity of solution supersaturation to critical supersaturation, which determined the dead zone width.[27]

It is shown[9] that supersaturation of sodium chlorate solution under investigated conditions practically depends only on supercooling. Since the significant difference between {100} growth rates of sodium chlorate crystals, which were grown at the same supersaturation yet different temperatures, does not exist in the observed temperature intervals, we analyzed (R,σ) dependence for {100} faces of individual crystals.

As is evident in Table 1, some of the {100} face growth rates versus supersaturation dependences can best be described by Chernov (3) and BFC (4) functions. Most of them (approximately 2/3) can best be described by one of the power functions $R \sim \sigma^n$ (6, 7, 8).

The solution temperature (supersaturation) was changed in the same manner for all crystals for the same type of experiments performed. The main conclusion that can be drawn from Table 1 and Figure 2 is the possibility that the individual crystal faces grew by different mechanisms under some conditions. Also, some additional conclusions based on presented results can be drawn:

(1) The growth of many {100} crystal faces can be described by the spiral growth mechanism. It refers to the faces pertaining to columns 3 and 4, and some of the faces pertain to columns 6, 7, and 8 whose power is $1 \leq n \leq 2$.
(2) Linear (n = 1) or parabolic (n = 2) growth rate versus supersaturation dependence existing for different faces, although they grew in the same supersaturation range.
(3) For many sodium chlorate crystals, in the experiments with a supersaturation decrease, the power (n) is higher than 2.
(4) Six to ten crystals, within error limits, in experiments with a supersaturation increase, grew with power $0.5 < n < 5/6$.

Table 1. Experimental Results

Eq	N	1a, 1b	2a, 2b	3	4	5	6	7	8	n (6, 7, 8)	$n \leq 2$	$n > 2$
σ_d	75	0	0	15	12	0	1	30	17	48	25	23
σ_i	85	0	0	7	15	5	16	6	36	58	56	2

https://doi.org/10.1021/acsomega.1c02150
ACS Omega 2021, 6, 21909−21914

(5) Only 5 of 160 crystal faces probably grew in the diffusion regime.

The simple power law is frequently used because of the difficulties in the use of eqs 1−7 for fitting experimental data. The behavior of all crystal faces, pertaining to columns 6, 7, and 8, whose power is $n > 2$, cannot be explained by existing crystal growth theories. Garside et al.[39] proposed that multiple nucleation is likely to hold, besides growing spirals, in this case.

It cannot be explained by the degree of neighboring step diffusion fields overlapping either. The behavior of all crystal faces, pertaining to columns 6, 7, and 8, whose power is $n > 2$, cannot be explained by this phenomenon. Namely, $n = 2$ for a small supersaturation ($\sigma \ll \sigma_c$) surface diffusion path is much smaller than the terrace width ($\lambda_s \ll \lambda$), and the diffusion fields are independent. In contrast, $n = 1$ for a high supersaturation ($\sigma \gg \sigma_c$) surface diffusion path is much higher than the terrace width ($\lambda_s \gg \lambda$), and diffusion fields overlap. Higher values of n correspond to smaller diffusion field overlapping of the neighboring steps.[38]

Coexistence of linear and parabolic dependence is impossible to explain by the diffusion fields overlap too. Namely, all crystals grew under the same conditions in the same type of the experiments performed—in the same interval of supersaturation. For all of them, only one or none of the mentioned conditions could be met, i.e., supersaturation cannot be both high and low at the same time.

We can only propose reasons for $n > 2$ in the power (R,σ) dependence. It is possible that the growth rate depends on more than two independent phenomena (events), which leads to the linear (R,σ) dependence. As is known, the probability of independent events is a product of their probabilities. It is also known that two independent events, the velocity of the steps and their density $(1/\lambda)$ both lead to linear (R,σ) dependence. Thanks to these phenomena, the (R,σ) dependence can occur with $1 \leq n \leq 2$. It is possible that more than two growth phenomena (events) presumed the power (R,σ) dependence with $n > 0$. If so, then the (R,σ) dependence will be a power function with the power higher than 2. Besides the velocity and density of the steps, these events can include point defects, a (random) distribution of dislocations (Frank network), the presence of grain boundaries and volume strain variations in the crystal,[14] electrical charge of the crystal face,[24] impurities, etc. Also, formation of inclusions during refaceting and further generation of dislocations might be responsible for different growth rates of crystals regenerated at different supersaturations.[40]

The stress back effect[41] and a special configuration of the growth spirals additionally complicate the (R,σ) dependence but do not presume the power law with $n > 2$.[31,32]

The fact that the power law, $R = K\sigma^n$, with $n > 2$ is applicable for sodium chlorate only when the supersaturation decreases confirms the assumption that the growth of sodium chlorate crystals depends on the growth history.[9,12] That the crystal growth depends on growth history is shown through the existence of crystal growth hysteresis—the crystal growth rate as the driving force (supersaturation or supercooling) increases is different from that when it decreases.[42−46] It is possible that this phenomenon causes differences in growth mechanisms in our experiments with the supersaturation increasing and decreasing.

The existence of crystal faces with $0.5 < n < 5/6$, in experiments with a supersaturation increase, indicates that these faces grew according to the two-dimensional mechanism, even corresponding data are better fitted by the power law (8) than the two-dimensional functions (1) and (2). This suggests that the polynuclear and multiple nuclear models for the two-dimensional nucleation compete. Hosoya and Kitamura[7] shown that sodium chlorate crystals grew by a two-dimensional mechanism in the supersaturation range of 3−5%. Our results have shown that rare faces can grow by this mechanism at small supersaturation (0.44−1.32%) too.

To date, the growth rate dispersion has been explained by the differences in growth parameters as presumed by the specific crystal growth theory. Our investigation showed that the growth rate dispersion might be a consequence of different growth mechanisms existing on equivalent crystal faces, i.e., a coexistence of different crystal growth mechanisms under the same experimental conditions is possible.

CONCLUSIONS

On the basis of the analysis of (R,σ) dependence for sodium chlorate crystal {100} faces, one may conclude that different faces of the same crystal could grow with different mechanisms under the same experimental conditions. Many of these crystal faces can be described by the spiral growth mechanism. The majority of the observed {100} sodium chlorate crystal faces grew in accordance with the power law $R \sim \sigma^n$ with $n \leq 2$, about 52% in experiments with a supersaturation decrease and about 97% in experiments with a supersaturation increase. The power dependence $R = K\sigma^n$ with $n > 2$ occurred for about 48% of {100} sodium chlorate crystal faces, in experiments with a supersaturation decrease. It is suggested that more independent phenomena and not only velocity and density of steps affect the face growth.

EXPERIMENTAL PROCEDURE

The idea behind experiments was to determine the correlation between the {100} face growth rates of sodium chlorate crystals and the solution supersaturation. The relative solution supersaturation is defined as $\sigma = (c - c_0)/c_0$, where c is the concentration and c_0 is the saturated solution concentration. The concentrations were calculated using the empirical formula[47]

$$c_0 = 0.226t + 44.38 \text{ (g NaClO}_3\text{/100 g solution)}$$

where t is the temperature of the solution.

Crystals were grown in a cylindrical cell (diameter 36 mm, height 15 mm). A detailed description of a crystallization cell in which crystals were nucleated and grown was described in ref 48. Crystals were nucleated by introducing air bubbles into the cell until small crystals appeared at the bottom. A transmitted light microscope was used to measure {100} crystal face displacement (accuracy of ±5 μm). The solution flow rate through the cell (capacity 15 mL) was about 0.5 mL/s. The velocity of the solution around the crystals, at the bottom of the cell, was about 0.05 mm/s. The solution temperature in the cell was kept constant within ±0.02 °C. We had three experimental runs for the supersaturation increase and also for the supersaturation decrease. During each growth run, 15−35 crystals were observed. Only crystals which did not intergrow with neighbor crystals on all five measured supersaturations were used for analysis. In all experiments, a solution saturated at 31.0 ± 0.1 °C was used, and nucleation was performed at 29.0 °C. At this temperature, crystals grew

https://doi.org/10.1021/acsomega.1c02150
ACS Omega 2021, 6, 21909−21914

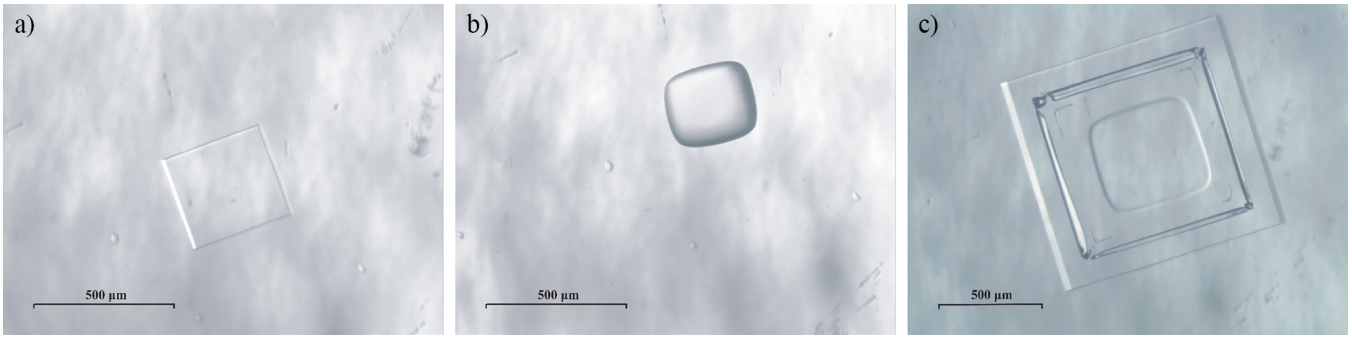

Figure 4. Sodium chlorate crystal: (a) before dissolution (non-dissolved), (b) after dissolution (partially dissolved), and (c) refaceted.

for about 2 h (Figure 4a). Then, the solution temperature was slowly increased to 34.0 ± 0.1 °C, approximately 0.5 °C/min. In about 25 min, the crystals were partially dissolved, at least 20% in the ⟨100⟩ direction (Figure 4b). Undissolved crystals were used as seeds for further growth in two types of experiments; the first with a solution supersaturation decrease and the second with a supersaturation increase. Both types of experiments were carried out in the supersaturation range of 0.44−1.32%.

In the first type of experiments with a supersaturation decrease, the solution with partially dissolved crystals was rapidly cooled to 28.0 °C followed by a temperature increase to 30.0 °C. In the second type of experiments with a supersaturation increase, the solution was rapidly cooled to 30.0 °C followed by a temperature decrease to 28.0 °C. The temperature is changed within 5 min in steps of 0.5 °C. At the first temperature reached after cooling, crystals were refaceted for about 30 min. Visible seeds' borders enabled measurements of face displacement, i.e., growth rates in the ⟨100⟩ directions (Figure 4c).

To stabilize the growth conditions (constant supersaturation), the solution was kept for about 15 min at each growth temperature, prior to growth rate measurements. The average growth rate in the ⟨100⟩ directions for each supersaturation was determined by the least-squares method. To provide a growth rate measurement error smaller than 3%, measurements lasted 1−3 h, depending on supersaturation.

AUTHOR INFORMATION

Corresponding Author

Mićo M. Mitrović − *University of Belgrade − Faculty of Physics, 11000 Belgrade, Serbia;* orcid.org/0000-0003-0646-8731; Email: mico@ff.bg.ac.rs

Authors

Biljana Z. Maksimović − *University of Belgrade − Faculty of Physics, 11000 Belgrade, Serbia*

Branislava M. Vučetić − *University of Belgrade − Faculty of Physics, 11000 Belgrade, Serbia*

Milica M. Milojević − *University of Belgrade − Faculty of Physics, 11000 Belgrade, Serbia*

Andrijana A. Žekić − *University of Belgrade − Faculty of Physics, 11000 Belgrade, Serbia;* orcid.org/0000-0001-7720-5846

Complete contact information is available at: https://pubs.acs.org/10.1021/acsomega.1c02150

Notes

The authors declare no competing financial interest.

ACKNOWLEDGMENTS

This work was supported by the Serbian Ministry of Education, Science and Technological Development through Grant No. 451-03-9/2021-14/200162.

NOTATION (NOMENCLATURE)

β_i^* - kinetic coefficient for steps
β - kink retardation factor
γ - surface free energy
ΔG_p^* - free energy change, corresponding to the formation of a stable circular nucleus on the perfect surface
λ_s - surface diffusion path
λ - terrace width
Λ - step retardation factor
σ - relative solution supersaturation
σ_c - critical value of relative solution supersaturation
Ω - specific molecular volume of growth units
A - surface area
b - size of the growth unit in the y direction
C, C', B, B^*, C^*, C_1, C_2, C_3, and K - growth constants
D_s - diffusion coefficient
h - height of steps of the nuclei
J - rate of two-dimensional nucleation
k - Boltzmann's constant
m - number of cooperating spirals in the dominant dislocation group with perimeter 2 L
n - supersaturation exponent
N_0 - concentration of growth units at the crystal surface
R - linear growth rate
T - temperature
v - nuclei step displacement rate

REFERENCES

(1) Bennema, P. Crystal Growth Measurements on Potassium Aluminium Alum and Sodium Chlorate from Slightly Supersaturated Solutions. *Phys. Status Solidi (b)* **1966**, *17*, 563−570.

(2) Koutsopoulos, S. Kinetic Study on the Crystal Growth of Hydroxyapatite. *Langmuir* **2001**, *17*, 8092−8097.

(3) Janssen-van, R. R.; Bennema, P.; Garside, J. The influence of volume diffusion on crystal growth. *J. Cryst. Growth* **1975**, *29*, 342−352.

(4) Denk, E. G., Jr.; Botsaris, G. D. Mechanism of potassium alum crystal growth from solution. *J. Cryst. Growth* **1970**, *6*, 241−244.

(5) Kim, S.; Myerson, A. S. Metastable solution thermodynamic properties and crystal growth kinetics. *Ind. Eng. Chem. Res.* **1996**, *35*, 1078−1084.

(6) Ristic, R.; Sherwood, J. N.; Wojciechowski, K. Morphology and growth kinetics of large sodium chlorate crystals grown in the presence and absence of sodium dithionate impurity. *J. Phys. Chem.* **1993**, *97*, 10774−10782.

(7) Hosoya, S.; Kitamura, M. In-situ observation of recovery process from rounded to faceted morphology in $NaClO_3$. *Mineral. J.* **1978**, *9*, 137−146.
(8) Surender, V.; Arundhathi, N.; Rao, K. K. Growth mechanism of $NaClO_3$ and $NaBrO_3$ crystals from aqueous solutions. *Bull. Mater. Sci.* **2006**, *29*, 427−432.
(9) Radiša, B. Z.; Mitrović, M. M.; Misailović, B. M.; Žekić, A. A. Investigation of growth mechanisms of sodium chlorate crystals from aqueous solutions. *Ind. Eng. Chem. Res.* **2016**, *55*, 10436−10444.
(10) Dincer, T. D.; Ogden, M. I.; Parkinson, G. M. Investigation of growth rate dispersion in lactose crystallisation by AFM. *J. Cryst. Growth* **2014**, *402*, 215−221.
(11) Ochsenbein, D. R.; Schorsch, S.; Salvatori, F.; Vetter, T.; Morari, M.; Mazzotti, M. Modeling the facet growth rate dispersion of β l-glutamic acid-Combining single crystal experiments with *n*D particle size distribution data. *Chem. Eng. Sci.* **2015**, *133*, 30−43.
(12) Pantaraks, P.; Flood, A. E. Effect of Growth Rate History on Current Crystal Growth: A Second Look at Surface Effects on Crystal Growth Rates. *Cryst. Growth Des.* **2005**, *5*, 365−371.
(13) Jones, C. M.; Larson, M. A. Characterizing growth-rate dispersion of $NaNO_3$ secondary nuclei. *AIChE J.* **1999**, *45*, 2128−2135.
(14) van der Heijden, A. E. D. M.; van der Eerden, J. P. Growth rate dispertion: the role of lattice strain. *J. Cryst. Growth* **1992**, *118*, 14−26.
(15) Zacher, U.; Mersmann, A. The influence of internal crystal perfection on growth rate dispersion in a continuous suspension crystallizer. *J. Cryst. Growth* **1995**, *147*, 172−180.
(16) Flood, A. E. Feedback between crystal growth rates and surface roughness. *CrystEngComm* **2010**, *12*, 313−323.
(17) Galbraith, S. C.; Flood, A. E.; Rugmai, S.; Chirawatkul, P. Relationship between Surface Roughness, Internal Crystal Perfection, and Crystal Growth Rate. *Chem. Eng. Technol.* **2016**, *39*, 199−207.
(18) Threlfall, T. L.; Coles, S. J. A perspective on the growth-only zone, the secondary nucleation threshold and crystal size distribution in solution crystallisation. *CrystEngComm* **2016**, *18*, 369−378.
(19) Srisanga, S.; Flood, A. E.; Galbraith, S. C.; Rugmai, S.; Soontaranon, S.; Ulrich, J. Crystal Growth Rate Dispersion versus Size-Dependent Crystal Growth: Appropriate Modeling for Crystallization Processes. *Cryst. Growth Des.* **2015**, *15*, 2330−2336.
(20) Jaho, S.; Athanasakou, G. D.; Sygouni, V.; Lioliou, M. G.; Koutsoukos, P. G.; Paraskeva, C. A. Experimental Investigation of Calcium Carbonate Precipitation and Crystal Growth in One- and Two-Dimensional Porous Media. *Cryst. Growth Des.* **2016**, *16*, 359−370.
(21) Martins, P. M.; Rocha, F. New developments on size-dependent growth applied to the crystallization of sucrose. *Surf. Sci.* **2007**, *601*, 5466−5472.
(22) Virone, C.; ter Horst, J. H.; Kramer, H. J. M.; Jansens, P. J. Growth rate dispersion of ammonium sulphate attrition fragments. *J. Cryst. Growth* **2005**, *275*, e1397−e1401.
(23) Wierzbowska, B.; Piotrowski, K.; Koralewska, J.; Matynia, A.; Hutnik, N.; Wawrzyniecki, K. Crystallization of vitamin C in a continuous DT MSMPR crystallizer − Size independent growth kinetic model approach. *Cryst. Res. Technol.* **2008**, *43*, 381−389.
(24) Sahin, Ö.; Bulutcu, A. N. Effect of surface charge distribution on the crystal growth of sodium perborate tetrahydrate. *J. Cryst. Growth* **2002**, *241*, 471−480.
(25) Alexandru, H. V.; Antohe, S. Prismatic faces of KDP crystal, kinetic and mechanism of growth from solutions. *J. Cryst. Growth* **2003**, *258*, 149−157.
(26) Mitrović, M. M.; Žekić, A. A.; Misailović, B. M.; Radiša, B. Z. Effect of Dissolution and Refaceting on Growth Rate Dispersion of Sodium Chlorate and Potassium Dihydrogen Phosphate Crystals. *Ind. Eng. Chem. Res.* **2014**, *53*, 19643−19648.
(27) Misailović, B. M.; Malivuk, D. A.; Žekić, A. A.; Mitrović, M. M. Nongrowing Faces of Sodium Chlorate Crystals in Supersaturated Solution. *Cryst. Growth Des.* **2014**, *14*, 972−978.
(28) Chernov, A. A.; Givargizov, E. I.; Bagdasarov, H. S.; Kuznetsov, V. A.; Demjancev, L. N.; Lobachev, A. N. *Crystal Growth (Modern Crystallography III), Springer Series in Solid State Sciences*; Springer: Berlin, 1984.
(29) Burton, W. K.; Cabrera, N.; Frank, F. C. The growth of crystals and the equilibrium structure of their surfaces. *Philos. Trans. R. Soc. A Math. Phys. Eng. Sci.* **1951**, *243*, 299−358.
(30) Bennema, P. Analysis of crystal growth models for slightly supersaturated solutions. *J. Cryst. Growth* **1967**, *1*, 278−286.
(31) Bennema, P. The importance of surface diffusion for crystal growth from solution. *J. Cryst. Growth* **1969**, *5*, 29−43.
(32) Bennema, P.; Gilmer, G. H. In: *Crystal Growth: An Introduction*; Hartman, P. (Ed.), North-Holland, Amsterdam, 1973.
(33) Markov, I. V. *Crystal Growth for Beginners − fundamentals of nucleation, crystal growth and epitaxy*; World Scientific Publishing Co. Pte. Ltd.: Singapore 2003.
(34) Sangwal, K. Growth kinetics and surface morphology of crystals grown from solutions: Recent observations and their interpretations. *Prog. Cryst. Growth Charact. Mater.* **1998**, *36*, 163−248.
(35) Spiegel, M. R. *Theory and Problems of Statistics, Principles and Method*; Wiley: New York, 1970.
(36) Lee, A.; Erdemir, D.; Myerson, A. S. Crystals and Crystal Growth. In *The Handbook of Industrial Crystallization*; 3rd ed.; Myerson, A. S.; Erdemir, D.; Lee, A.; Eds.; Cambridge University Press: Cambridge, U.K., 2019; pp. 32−75.
(37) *Crystallisation*; 4th Edition By Mullin, J. W. 2001. Butterworth Heinemann: Oxford, UK.
(38) Bennema, P.; Boon, J.; Van Leeuwen, C.; Gilmer, G. H. Confrontation of the BCF Theory and Computer Simulation Experiments with Measured (R, σ) Curves. *Krist. Tech.* **1973**, *8*, 659−678.
(39) Garside, J.; Janssen-van Rosmalen, R.; Bennema, P. Verification of crystal growth rate equations. *J. Cryst. Growth* **1975**, *29*, 353−366.
(40) Wojciechowski, K. Growth Rates Of Sodium Chlorate Crystals Grown From Aqueous Solution In Relation To Internal Strain. *Cryst. Res. Technol.* **1999**, *34*, 661−666.
(41) Cabrera, N.; Coleman, R. V. *The Art and Science of Growing Crystals*; In: Gilman, J. J. (Ed.), John Wiley & Sons.: New York, 1963.
(42) Miura, H. Crystal Growth Hysteresis in Spiral Growth. *Cryst. Growth Des.* **2020**, *20*, 245−254.
(43) Friddle, R. W.; Weaver, M. L.; Qiu, S. R.; Wierzbicki, A.; Casey, W. H.; De Yoreo, J. J. Subnanometer atomic force microscopy of peptide−mineral interactions links clustering and competition to acceleration and catastrophe. *Proc. Natl. Acad. Sci. U. S. A.* **2010**, *107*, 11−15.
(44) Guzman, L. A.; Kubota, N.; Yokota, M.; Sato, A.; Ando, K. Growth hysteresis of a potassium sulfate crystal in the presence of chromium(III) impurity. *Cryst. Growth Des.* **2001**, *1*, 225−229.
(45) Dugua, J.; Simon, B. Crystallization of sodium perborate from aqueous solutions. *J. Cryst. Growth* **1978**, *44*, 280−286.
(46) Land, T. A.; Martin, T. L.; Potapenko, S.; Polmore, G. T.; De Yoreo, J. J. Recovery of surfaces from impurity poisoning during crystal growth. *Nature* **1999**, *399*, 442−445.
(47) Ristić, R.; Shekunov, B. Y.; Sherwood, J. N. Growth of the tetrahedral faces of sodium chlorate crystals in the presence of dithionate impurity. *J. Cryst. Growth* **1994**, *139*, 336−343.
(48) Malivuk, D. A.; Žekić, A. A.; Mitrović, M. M.; Misailović, B. M. Dissolution of sodium chlorate crystals in supersaturated solutions. *J. Grys. Growth* **2013**, *377*, 164−169.

https://doi.org/10.1021/acsomega.1c02150
ACS Omega 2021, 6, 21909−21914